The Canadian Mineralogist
Vol. 47, pp. 303-314 (2009)
DOI: 10.3749/canmin.47.2.303

THE CRYSTAL CHEMISTRY OF THE KORNERUPINE–PRISMATINE SERIES. V. THE SITE OF BERYLLIUM IN KORNERUPINE

Mark A. COOPER and Frank C. HAWTHORNE[§]

Department of Geological Sciences, University of Manitoba, Winnipeg, Manitoba R3T 2N2, Canada

Edward S. GREW

Department of Earth Sciences, University of Maine, Orono, Maine 04469, U.S.A.

Abstract

The crystal structure of a sample of Be-bearing kornerupine, *Cmcm, a* 16.040(6), *b* 13.671(3), *c* 6.704(2) Å, *V* 1470.1(8) Å^3, $Z = 4$, has been refined to an *R* index of 3.4% based on 1201 unique observed ($|F_o| > 4\sigma F$) reflections measured with graphite-monochromated Mo*K*α X-radiation. Prior to collection of the X-ray data, the crystal used was analyzed with an electron microprobe and SIMS to give the unit formula $Na_{0.014}\,Mg_{3.452}\,Fe^{2+}{}_{0.169}\,Fe^{3+}{}_{0.234}\,Al_{5.933}\,Be_{0.200}\,B_{0.430}\,Si_{3.888}\,O_{21}\,(OH)$, where B and Fe^{2+}/Fe^{3+} were derived according to the procedure established in the companion paper. Site-scattering refinement and stereochemical considerations show that Be is restricted to the *T*(3) site, which has the following site-population: 0.23 Si + 0.14 Al + 0.43 B + 0.20 Be. The presence of Be can be deduced directly from the results of crystal-structure refinement. The Be content derived by site-scattering refinement is in exact accord with the content analyzed by SIMS. Local bond-valence arguments suggest that there is extensive short-range order around the Be atom at the *T*(3) site, with the locally adjacent *T*(2) sites being occupied by Si.

Keywords: kornerupine, Be-bearing, crystal-structure refinement, site populations, local bond-valence requirements, short-range order.

Sommaire

Nous avons affiné la structure cristalline d'un échantillon de kornérupine contenant du béryllium, *Cmcm, a* 16.040(6), *b* 13.671(3), *c* 6.704(2) Å, *V* 1470.1(8) Å^3, $Z = 4$, jusqu'à un résidu *R* de 3.4% en utilisant 1201 réflexions uniques observées ($|F_o| > 4\sigma F$) mesurées en diffraction X avec rayonnement Mo*K*α et monochromatisation par le graphite. Avant la collection de ces données, nous avons analysé le cristal avec une microsonde électronique et par spectrométrie de masse des ions secondaires (SIMS), ce qui a donné la formule $Na_{0.014}\,Mg_{3.452}\,Fe^{2+}{}_{0.169}\,Fe^{3+}{}_{0.234}\,Al_{5.933}\,Be_{0.200}\,B_{0.430}\,Si_{3.888}\,O_{21}\,(OH)$, dans laquelle la teneur en B et Fe^{2+}/Fe^{3+} sont dérivés selon la procédure établie dans notre travail antérieur. L'affinement de la dispersion associée aux sites et les considérations stéréochimiques montrent que le Be n'occupe que le site *T*(3), où logent 0.23 Si + 0.14 Al + 0.43 B + 0.20 Be. Nous pouvons déduire la présence de Be directement à partir des résultats de l'affinement de la structure. La teneur en Be dérivée par affinement de la dispersion au site *T*(3) concorde exactement avec la teneur établie par SIMS. A partir des arguments à propos des valences de liaison locales, une mise en ordre à courte échelle est développée autour de l'atome Be au site *T*(3), les sites *T*(2) adjacents étant occupés par Si.

(Traduit par la Rédaction)

Mots-clés: kornérupine, contenu de Be, affinement de la structure, populations des sites, exigeances locales des valences de liaison, mise en ordre à courte échelle.

[§] E-mail address: frank_hawthorne@umanitoba.ca

INTRODUCTION

The kornerupine–prismatine series, $(\square,\mathrm{Mg,Fe})(\mathrm{Al,Mg,Fe})_9(\mathrm{Si,Al,B})_5\mathrm{O}_{21}(\mathrm{OH,F})$, is a favorable host for Be and incorporates it as readily as the better known "sinks" for Be, cordierite and sapphirine (*e.g.*, Grew 1996, 2002, Grew *et al.* 1990a, 1998, 2003). The highest contents of Be reported in this series are 0.32 and 0.74 wt.% BeO (corrected for revision in Be content of surinamite standard used for SIMS analysis) in kornerupine from whiteschists from Mulvoj, southwestern Pamirs, Tajikistan (Grew *et al.* 1990b, 1998) and Chilapila Hill, Lufilian arc, Zambia (Vrána & Barr 1972), respectively. Given the absence of a Be-saturating phase in these whiteschists, it is likely that kornerupine–prismatine could incorporate significantly more Be. However, an attempt to synthesize a B-free Be analogue at 780°C, 6 kbar using a starting composition $\mathrm{Mg}_{3.5}\,\mathrm{Al}_6\,\mathrm{Be}_{0.5}\,\mathrm{Si}_4\,\mathrm{O}_{20}\,(\mathrm{OH})_2$ produced only a trace of kornerupine among the products (Hölscher 1987). In order to understand the mechanisms for incorporation of Be in kornerupine, the Chilapila Hill sample (8HC 161, denoted here as K53) was investigated in detail; Grew *et al.* (1998) reported 1.86 wt.% $\mathrm{B_2O_3}$ and 0.74 wt.% BeO by SIMS.

The chemical composition of K53 is relatively simple, in that there are only six elements (ignoring Be for the moment) (B, Na, Mg, Al, Si, Fe) to assign to the various cation sites. Complexity arises from the fact that there are a large number of sites over which to assign these elements (three tetrahedrally coordinated *T*-sites, five octahedrally coordinated *M*-sites, and an [8]-coordinated *X*-site). Further complicating the task of assigning cations to these sites are the following issues: (i) the Fe^{2+}:Fe^{3+} ratio needs to be derived, (ii) the B content needs to be extracted from site-scattering arguments, (iii) Al is distributed over both *M* and *T* sites, and (iv) the total number of cations is unknown, as there is significant vacancy present at the *X* site. From the study of 47 well-refined kornerupine crystals, Cooper *et al.* (2009a) were able to show well-resolved site-populations for all cation sites. The kornerupine crystal in this study was initially analyzed by SIMS and contains 0.74 wt.% BeO (Grew *et al.* 1998). We present here the results of combined crystal-structure refinement (SREF), electron-microprobe analysis (EMPA) and secondary-ion mass spectrometry (SIMS) on this crystal. These results are then compared with those of the earlier study on kornerupine (Cooper *et al.* 2009a, b) with the following questions in mind: (1) Is it possible to identify which of the three *T* sites carries the Be? (2) Assuming initially that Be is absent, can its presence be inferred from electron-microprobe (EMP) and structure-refinement (SREF) results? (3) Is it possible to estimate the Be content from SREF and EMPA alone?

TABLE 1. MISCELLANEOUS INFORMATION FOR KORNERUPINE K53

a (Å)	16.040(6)	crystal size (μm)	25 × 55 × 60
b	13.671(3)	radiation	Mo*K*α/Graphite
c	6.704(2)	No. of reflections	1201
V (Å^3)	1470.1(8)	No. observed	1201
Space group	*Cmcm*	No. $\lvert F_o\rvert > 4\sigma\lvert F\rvert$	737
Z	4	R_1 ($\lvert F_o\rvert > 4\sigma$) %	3.4
		wR_2 (F_o^2) %	6.4

EXPERIMENTAL

A rectangular fragment of kornerupine (Table 1) was removed from a thin section, attached to a glass fiber and mounted on a Bruker four-circle single-crystal diffractometer. Twenty-five reflections were centered, and the unit-cell parameters (Table 1) were refined by least squares from the resultant setting angles. Intensity data were collected in θ–2θ scan-mode at a fixed scan-rate of 0.8° 2θ/min. A total of 1201 reflections was measured to 60° 2θ over one asymmetric unit. A total of 180 psi-scan intensities was collected for five strong reflections at intervals of 10° about the diffraction vector, and a subsequent absorption-correction reduced *R*(azimuthal) from 1.2 to 0.9%. The normal intensity-data were corrected for absorption, Lorentz, polarization and background effects, and reduced to structure factors; of the 1201 unique reflections, all 1201 were considered as observed ($F_o^2 > 3(\sigma/2)F^2$ for wR_2, and 737 were considered as observed ($\lvert F_o\rvert > 4\sigma F$) for R_1. The Bruker SHELXTL (PC version) system of programs was used throughout this study. Scattering curves for neutral atoms (metals) were taken from Ibers & Hamilton (1992) and for ionized oxygen (O^{2-}) from Azavant & Lichanot (1993). Full-matrix least-squares refinement (based on F_o^2 and all 1201 unique data) of all variable parameters for a model involving anisotropic displacement of all non-H atoms converged to an R_1 index of 3.4% for 737 observed unique reflections ($\lvert F_o\rvert > 4\sigma F$). A weighting scheme suggested by the program gave $wR_2 = 6.4\%$. These *R* values are somewhat high relative to those of Cooper *et al.* (2009a). We attribute this (in part) to the appreciably smaller crystal used in this study, and the fact that the crystal was in part damaged by previous SIMS analysis. The chemical composition was measured before the single-crystal structure study (Grew *et al.* 1998) and is given in Table 2.

CRYSTAL-STRUCTURE REFINEMENT

Initial refinement of the structure

We began by assuming that the *T* sites are occupied by (Si + Al) at *T*(1) and *T*(2), and by (Si + Al + B) at *T*(3). The initial refinement was done with Si and B assigned to the *T*(3) site, with a free variable constraining the sum of the site occupancies to full occupancy. The site-scattering values at the *X, M*(1), *M*(2), *M*(4) and *T*(2) sites were refined, and those at the *M*(3), *M*(5) and *T*(1) sites were constrained in the manner shown in Table 3. Cooper *et al.* (2009a) showed that this initial refinement-model produces good starting estimates of B and Fe^{3+} contents [because B and Fe^{3+} are ordered at the *T*(3) and *M*(4) sites, respectively]. These initial B and Fe^{3+} values were then used to normalize the EMP data. In this manner, a more accurate assessment of Si content was derived. Then, using the <*T*–O> *versus* constituent-radii plots of Cooper *et al.* (2009a), Si and Al populations were derived for the *T*(1) and *T*(2) sites from the observed <*T*(1)–O> and <*T*(2)>–O> distances. After Si was assigned to *T*(1) and *T*(2) in this manner, all remaining Si was assigned to *T*(3). An initial Al-content at *T*(3) was then derived by difference. The refinement model was then modified to have fixed occupancies of Si and Al at *T*(1) and *T*(2), and a fixed Al content was assigned to *T*(3). The coupled Si and B site-occupancies at the *T*(3) sites were refined to fine-tune the B value derived from the initial structure-refinement. The formula calculation was then updated with the new B and Fe^{3+} values, and the process was iterated until the refined quantities [B, Fe^{3+} occupancies; <*T*(1)–O>, <*T*(2)–O> bond lengths] showed no change. After the third update in the refinement model, the process had iterated to completion; the B and Fe^{3+} values had changed from their initial starting values of 0.653 and 0.236 *apfu*, to 0.644 and 0.234 *apfu*, respectively. The *T* site-populations, calculated constituent-radii and mean observed bond-lengths are given in Table 4. In Figure 1, the data of Cooper *et al.* (2009a) are plotted as black circles; the data for Be-bearing kornerupine K53 are plotted as white squares and emphasized by dotted lines. The data for *T*(1) and *T*(2) in K53 were constrained to agree with the relations for the *T*(1) and *T*(2) sites (black lines), with the result that the data for *T*(3) in K53 are significantly displaced from the relation for the *T*(3) site in Be-free kornerupine (Cooper *et al.* 2009a). If the tetrahedra in K53 contain only (Si + Al + B), how can one explain these results relative to those of Cooper *et al.* (2009a)? It might be argued that the displacement of the data point on the *T*(3) plot from the ideal line has been exaggerated, in that the data points were forced to fit the *T*(1) and *T*(2) plots. However, it is shown in Appendix A that it is not possible to produce an Si–Al–B distribution over the *T*(1), *T*(2) and *T*(3) sites that is conformable with established site-populations in kornerupine. Hence we deduce that a significant amount of a fourth component *must* be present at the *T* sites.

Introduction of a fourth tetrahedrally coordinated component

The SIMS analysis of this specific sample of kornerupine indicates that significant Be could be the perturbing influence on the tetrahedra (Table 2). To help identify the *T* site(s) at which Be is located, both its site-scattering "signature" and effective radius need to be considered, relative to the other *T*-site substituents (Table 5). If Be were located at *T*(1) or *T*(2), the most sensitive means of detecting minor quantities in the crystal-structure refinement is *via* a noticeable reduction in the observed site-scattering. There are two important considerations regarding the quantitative assessment of Be *via* observed site-scattering values at *T*(1) and *T*(2):

(1) *T*(1) and *T*(2) are 8*g* sites, and each hosts two tetrahedrally coordinated cations *pfu*. The Be content from SIMS analysis is only 0.2 *apfu*. How sensitive are the refined site-scattering values to such minor substitution of Be?

TABLE 2. CHEMICAL COMPOSITION* AND UNIT FORMULA OF KORNERUPINE K53

SiO_2 wt.%	31.55	Si *apfu*	3.888
Al_2O_3	40.85	B	0.430
MgO	18.79	Be	0.200
Na_2O	0.06	$^{[4]}Al$	0.482
FeO *	1.64	Σ*T*	5.000
Fe_2O_3 *	2.52		
BeO *	0.68	$^{[6]}Al$	5.451
B_2O_3 *	2.02	Fe^{3+}	0.234
H_2O **	1.22	$^{[6]}Mg$	3.146
		Fe^{2+}	0.169
Total	99.33	Σ*M*	9.000
		$^{[8]}Mg$	0.306
		Na	0.014
		Σ*X*	0.320
		H	1.000

* FeO, Fe_2O_3, BeO and B_2O_3 values were calculated from the Fe^{2+}, Fe^{3+}, Be and B values derived from crystal-structure refinement; other values are from Grew *et al.* (1998). ** Calculated assuming OH = 1.00 *apfu* (Cooper *et al.* 2009b) and 22 anions *pfu*.

TABLE 3. SITE-SCATTERING ASSIGNMENTS AT DIFFERENT STAGES OF THE REFINEMENT OF KORNERUPINE K53

	1*		2*		3*
X	Mg, [Na]	→ +			
M(1)	Mg, Fe	→			
M(2)	Mg, Fe	→			
M(3)	[Al] **	→			
M(4)	Al, Fe	→			
M(5)	[Al]	→			
T(1)	[Si]		[Si] [Al]	→	
T(2)	Si		[Si] [Al]	→	
T(3)	Si, B		Si, B [Al]		Si, B, [Al] [Be]

* Denotes first, second and third stages of refinement; ** [A] denotes fixed occupancy of A; A denotes variable occupancy of A; + the arrows indicate that the same assignments are used in the following stages of refinement.

TABLE 4. INITIAL ASSIGNED SITE-POPULATIONS (*apfu*) AT THE *T* SITES FOR KORNERUPINE K53

	Si	Al	B	r (Å)	<*T*–O> (Å)
T(1)	1.953	0.047	–	0.263	1.621
T(2)	1.705	0.295	–	0.279	1.652
T(3)	0.207	0.149	0.644	0.183	1.587

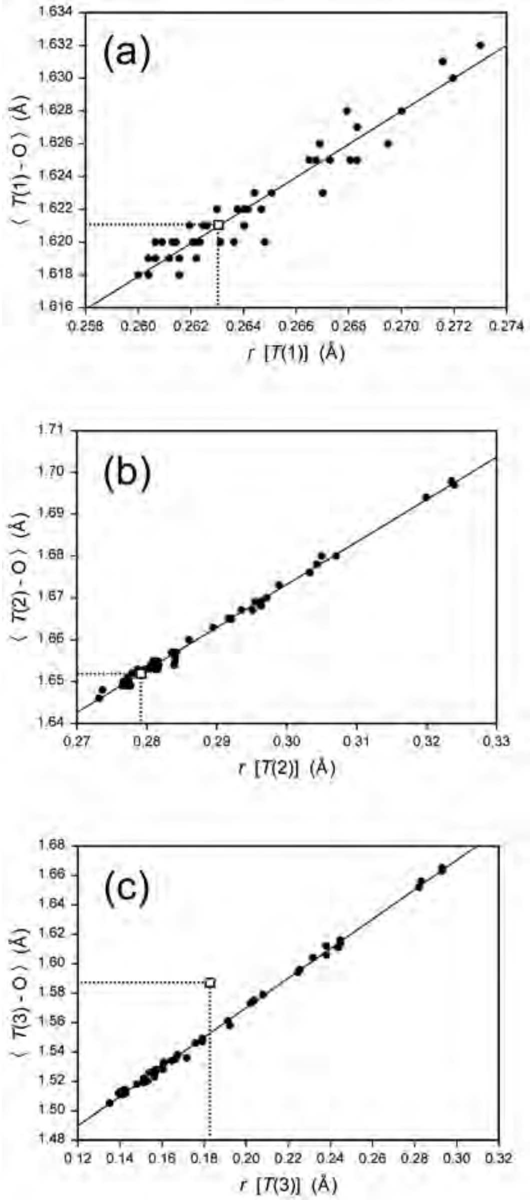

FIG. 1. The variation in <*T*–O> distances as a function of constituent-cation radius for the data of Cooper *et al.* (2009a) (black circles) and for K53 (white square); also shown are the regression lines of Cooper *et al.* (2009a); the dotted lines emphasize the position of the data points for K53; (a) the *T*(1) site; (b) the *T*(2) site; (c) the *T*(3) site. Note that in (a) and (b), the points for K53 are constrained to lie on the regression lines, with the result that the point for K53 in (c) is significantly displaced from the regression line.

(2) In refining crystal structures, we have observed the following characteristic behavior: where the site-scattering values at *all* cation sites are refined, the resulting site-scattering values tend to be too low. The nature of the kornerupine structure also complicates this issue by the fact that there are nine distinct cation sites (excluding H), and all show solid solution involving two or more elements (Cooper *et al.* 2009a). The refinement strategy of Cooper *et al.* (2009a) for forty-seven kornerupine crystals used constrained Si–Al site-occupancies for the *T*(1) and *T*(2) sites in order to help alleviate the problem of site-scattering values refining too low. If the site occupancies for the *T*(1) and *T*(2) sites in K53 are allowed to refine, we anticipate that they would refine to values that are too low. So how does one determine whether the reduction in refined site-scattering is due to the presence of minor Be, or has resulted from simultaneous site-scattering refinement at too many cation sites?

To better assess the occupancies at the *T*(1) and *T*(2) sites in K53, we re-refined the structures of all the kornerupine crystals of Cooper *et al.* (2009a) to investigate quantitatively the refinement behavior of the *T*(1) and *T*(2) occupancies. We considered two refinement models: (1) refining *T*(1) site-occupancy with fixed *T*(2) site-occupancy; (2) fixed *T*(1) site-occupancy and refining *T*(2) site-occupancy. In this manner, we were able to assess the refined occupancies at *T*(1) and *T*(2) in an independent manner. Figure 2 shows the assigned site-scattering values (from stereochemical considerations: Cooper *et al.* 2009a) at *T*(1) and *T*(2) as a function of their respective refined values. The total range in site-scattering values spans approximately 1 *epfu*, equal to a range in Si : Al of 1:0 to 0.50:0.50. The field of data approximate the slope of the 1:1 reference line, indicating good agreement between assigned and refined electrons at the two sites. The field of data is also displaced to the left of the reference line, showing the amount by which the occupancies have refined to too low a value (~0.2 electrons). The refined data for K53 (squares) are plotted on Figure 2, using the initial site-populations (Table 4) and the values refined in the same manner as those for the other 47 kornerupine crystals in Figure 2. The data for K53 plot within the respective *T*(1) and *T*(2) data fields, suggesting that the refined site-scattering is consistent with the assigned

TABLE 5. CONSTITUENTS OF TETRAHEDRA IN KORNERUPINE K53

	Si	Al	B	Be
electrons	14	13	5	4
radius (Å) *	0.26	0.39	0.11	0.27

* Shannon (1976).

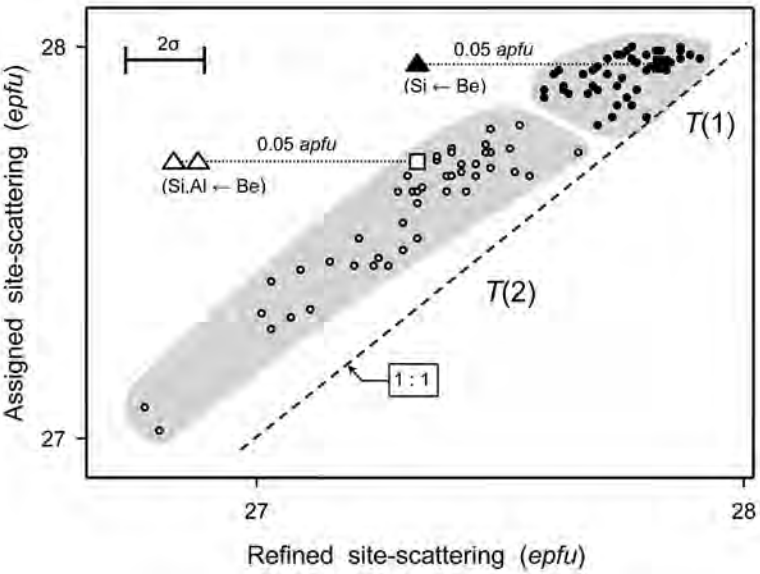

FIG. 2. The variation in assigned site-scattering as a function of refined site-scattering at the *T*(1) and *T*(2) sites for the data of Cooper *et al.* (2009a). Black circles: *T*(1) site, white circles: *T*(2) site; square: K53. Triangles mark hypothetical site-scattering for K53 assuming substitution of 0.05 *apfu* Be for Si at *T*(1) and for (Si,Al) at *T*(2). The dashed line marks the 1:1 reference line.

Si–Al content. Triangles in Figure 2 plot at positions that correspond to a hypothetical replacement of 0.05 *apfu* Be for Si at *T*(1), or (Si,Al) at *T*(2). The refined site-scattering values at *T*(1) and *T*(2) are clearly too large for any appreciable Be to occur at these sites. Moreover, significantly less than 0.05 *apfu* Be should be detectable at the *T*(1) and *T*(2) sites.

The T(3) site

As we have shown that the *T*(1) and *T*(2) sites do not contain significant Be, the Be established by SIMS *must* occur at the *T*(3) site. However it is desirable to assess the *T*(3) site directly with regard to possible Be content. As shown in Figure 1c, where only (B + Si + Al) is considered as constituents of *T*(3), the resulting aggregate radius is too small for the observed <*T*(3)–O> bond length. This observation is in accord with the occurrence of Be at *T*(3).

It is desirable to obtain site-scattering evidence as to the location of Be. To this end, we ran two more series of *T*-site-scattering refinements, where small quantities (0.1, 0.2 *apfu*) of Be were assigned to the *T*(3) site. The Be site-occupancy was fixed in the refinement, and the Si and B contents were refined. With the new refined B content derived from the refinement, the microprobe data were renormalized using this new B (and constrained Be) content. In this way, the Si content was partitioned amongst the *T* sites, and a fixed Al content could be assigned to *T*(3) by difference. By the third iteration of this procedure, there was no significant change in the refinement. The new *T*(3) site assignments, assuming 0.1 and 0.2 Be *apfu*, are given in Table 6, and the corresponding aggregate radii are plotted against the observed <*T*(3)–O> value of 1.587 Å in Figure 3. The data point corresponding to 0.2 Be *apfu* plots very near the established relation between aggregate radius and mean bond-length developed for the *T*(3) site (Cooper *et al.* 2009a), and the corresponding 0.68 wt.% BeO agrees with the 0.74 wt.% value from the results of the SIMS analysis (Table 2) within the 1σ reproducibility of ±10% estimated for the SIMS measurement (Grew *et al.* 2000).

M- and X-site assignment

Cations were assigned to the remaining sites using the site-assignment results of Cooper *et al.* (2009a) as a guide. The *M*(1) site is occupied solely by Mg and Fe^{2+}, and the site occupancies were calculated directly from the site-scattering results (Table 7). The *M*(2) and *M*(4) sites are occupied by Mg, Al and Fe. As Mg (Z = 12) and Al (Z = 13) have very similar X-ray scattering factors, we assigned (Mg + Al) and Fe site-occupancies from the refined site-scattering value (Table 7), and then the Mg and Al site-occupancies were assigned from the relevant aggregate-constituent-radius – bond-length relations of Cooper *et al.* (2009a). The *M*(3) and *M*(5) sites are occupied primarily by Al with minor Mg; the site occupancies were assigned from the relevant aggregate-constituent-radius bond-length relations of Cooper *et al.* (2009a). All remaining Mg, together with Na, was assigned to the *X* site.

This procedure resulted in a relatively small discrepancy between the Fe assigned from the refined site-scattering values (0.192 *apfu*) and that derived from the electron-microprobe composition (0.169 *apfu*). The Fe was proportionally reduced at the *M*(1) and *M*(2) sites to bring the total Fe in coincidence with the electron-microprobe value, and the Mg and Al contents at the *M*(2), *M*(3), *M*(4) and *M*(5) sites were adjusted so as to minimize the deviation from the <*M*–O> – aggregate-constituent-radius relations of Cooper *et al.* (2009a). The final site-populations are given in Table 7, together with the refined and calculated site-scattering values; in addition, Table 7 shows the observed mean bond-lengths and the corresponding values calculated from the relations of Cooper *et al.* (2009a). The largest difference between the observed and calculated site-scattering values (0.9 *epfu*) is for the *X* site; this difference falls within the limits of agreement of ±1 *epfu* for all kornerupine crystals of Cooper *et al.* (2009a).

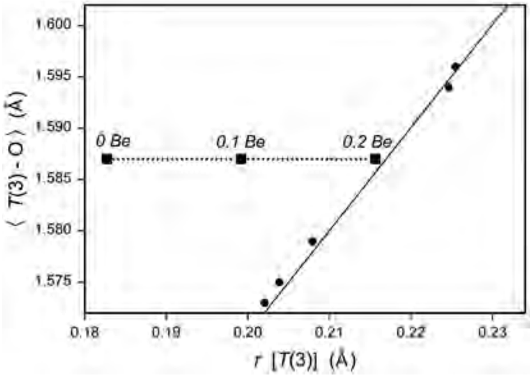

FIG. 3. The variation in <*T*(3)–O> as a function of constituent-cation radius for the data and regression line of Cooper et al. (2009a); only a small part of the overall variation is shown here (*cf.* Fig. 1c). The black squares are the relevant refined values for K53 assuming 0.0, 0.1 and 0.2 Be *apfu* at *T*(3), respectively.

Short-range order in Be-bearing kornerupine

The crystal-structure refinement of K53 showed that Be occupies the *T*(3) site. The *T*(3) site is usually occupied by Si, B and Al; Be has a formal charge of 2^+, whereas the normal constituents of *T*(3) have formal charges of 4^+ and 3^+. Hence the occurrence of Be at *T*(3) will result in considerable short-range order of cations at the next-nearest-neighbor sites in order that the local version of the valence-sum rule (Hawthorne 1997a) be satisfied. A representation of the salient part of the structure of kornerupine is shown in Figure 4. Of key importance with respect to local bond-valence satisfac-

TABLE 6. *T*(3) SITE-ASSIGNMENTS (*apfu*) FOR VARIOUS Be CONTENTS IN KORNERUPINE K53

	Si	Al	B	Be	*r* (Å)
0.0 Be	0.207	0.149	0.644	0	0.183
0.1 Be	0.219	0.144	0.537	0.1	0.199
0.2 Be	0.230	0.140	0.430	0.2	0.216

TABLE 7. FINAL SITE-POPULATIONS (*apfu*), SITE-SCATTERING VALUES (*epfu*) AND MEAN BOND-LENGTHS (Å) FOR KORNERUPINE K53

	Be	B	Si	Al	□	Na	Mg	Fe^{2+}	Fe^{3+}	e_{ref}*	e_{calc}	$<A–O>_{calc}$**	$<A–O>_{obs}$
T(1)			1.953	0.047						(28.0)	28.0	1.621	1.621
T(2)			1.705	0.295						(27.7)	27.7	1.652	1.652
T(3)	0.200	0.430	0.230	0.140						8.0	8.0	1.586	1.587
X					0.680	0.014	0.306			2.9	3.8	2.411	2.406
M(1)							1.885	0.115		25.8	25.6	2.118	2.113
M(2)				0.150			0.796	0.054		12.9	12.9	2.086	2.083
M(3)				1.929			0.071			(26.0)	25.9	1.926	1.925
M(4)				1.399			0.367		0.234	29.0	28.7	1.964	1.963
M(5)				1.973			0.027			(26.0)	26.0	1.913	1.912
	0.200	0.430	3.888	5.933	0.680	0.014	3.452	0.169	0.234				

* Values in parentheses were fixed during the final refinement; ** calculated using the relations of Cooper *et al.* (2009a).

TABLE 8. POSSIBLE SHORT-RANGE ARRANGEMENTS OF CATIONS AROUND O(7) AND O(8) IN Be-BEARING KORNERUPINE

O(7)						O(8)						
T(3)	*T*(2)	*M*(1)	Bond strengths (*vu*)		Code	*T*(3)	*M*(2)	*M*(5)	*M*(5)	Bond strengths (*vu*)		Code
Si	Si	Mg	1 + 1 + ⅓ =	2.33	**	Si	Al	Al	Al	1 + ½ + ½ + ½ =	2.50	
Si	Al	Mg	1 + ¾ + ⅓ =	2.08	*(*)	Si	Mg	Al	Al	1 + ⅓ + ½ + ½ =	2.33	**
B,Al	Si	Mg	¾ + 1 + ⅓ =	2.08	**	Si	Mg	Al	Mg	1 + ⅓ + ½ + ⅓ =	2.17	*
B,Al	Al	Mg	¾ + ¾ + ⅓ =	1.83	*(*)	Si	Mg	Mg	Mg	1 + ⅓ + ⅓ + ⅓ =	2.00	*
Be	Si	Mg	½ + 1 + ⅓ =	1.83	**	Al,B	Al	Al	Al	¾ + ½ + ½ + ½ =	2.25	*(*)
Be	Al	Mg	½ + ¾ + ⅓ =	1.58		Al,B	Mg	Al	Al	¾ + ⅓ + ½ + ½ =	2.08	**
						Al,B	Mg	Mg	Al	¾ + ⅓ + ⅓ + ½ =	1.92	*
						Al,B	Mg	Mg	Mg	¾ + ⅓ + ⅓ + ⅓ =	1.75	*
						Be	Al	Al	Al	½ + ½ + ½ + ½ =	2.00	*(*)
						Be	Mg	Al	Al	½ + ⅓ + ½ + ½ =	1.83	**
						Be	Mg	Mg	Al	½ + ⅓ + ⅓ + ½ =	1.67	*
						Be	Mg	Mg	Mg	½ + ⅓ + ⅓ + ⅓ =	1.50	

* feasible arrangement, *(*) limiting arrangement, ** favored arrangement.

tion are the O(7) and O(8) anions, which are coordinated by the *T*(3) + *T*(2) + *M*(1) and the *T*(3)–*M*(2)–*M*(5)–*M*(5) sites, respectively. It is immediately apparent that occupancy of *T*(3) by tetravalent (Si), trivalent (B,Al) and divalent (Be) cations should be coupled to occupancy of *T*(2), *M*(1), *M*(2) and *M*(5) by (Si,Al), (Mg), (Mg,Al) and (Al,Mg), respectively (including Fe^{2+} with Mg). A simple way to examine this issue is to consider the local (Pauling) bond-strengths incident at O(7) and O(8) for all possible short-range configurations of cations in terms of the valence-sum rule. These configurations and associated bond-strength values are shown in Table 8.

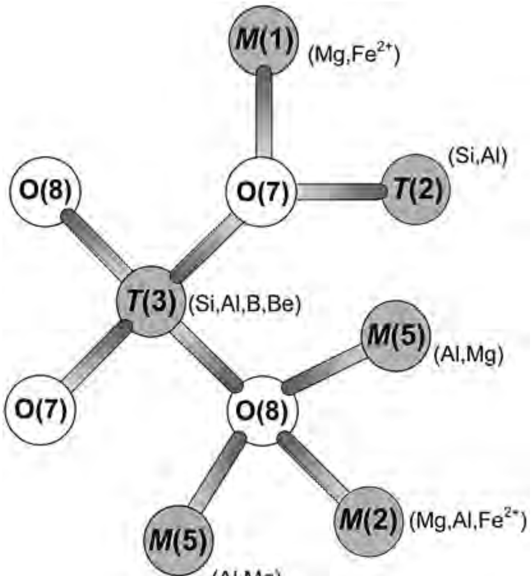

FIG. 4. Schematic view of part of the kornerupine structure around the O(7) and O(8) anions; cations are shown as grey circles, anions are shown as white circles.

Inspection of Table 8 shows that many of the geometrically possible arrangements of cations lead to incident bond-strength sums that depart significantly from the valence-sum rule. Those arrangements that are in reasonable accord with the valence-sum rule (*i.e.*, within $1.67 \le \Sigma \le 2.33$ *vu*) are marked by a * (Table 8). In addition, the observed site-populations (Table 7) are not in accord with some of the *-marked arrangements occurring in substantial amounts: for example, the amount of Mg at *M*(5) is very low (0.027 *apfu*, 0.014 atoms per site; Table 7), and hence configurations involving Mg at *M*(5) cannot occur in any significant number. All arrangements that are *not* affected by such compositional constraints [in terms of the *T*(3) constituent] are marked by a second *, and those that are partly limited are marked by a second (*) in parentheses (Table 8). Inspection of Table 8 shows that there is only one optimal short-range arrangement of cations around O(7) [*T*(3)–*T*(2)–*M*(1) = Be–Si–Mg] that involves Be at *T*(3), and two arrangements around O(8) [*T*(3)–*M*(2)–*M*(5)–*M*(5) = Be–Mg–Al–Al or Be–Al–Al–Al] that involves Be at *T*(3). Consider first the local arrangements involving O(7). For each Be atom at *T*(3), there are two Be–Si–Mg configurations (see Fig. 4); hence the overall cluster is $^{M(1)}$Mg–$^{T(2)}$Si–$^{T(3)}$Be–$^{T(2)}$Si–$^{M(1)}$Mg, and there are 0.200 *pfu* such local clusters. Similarly, for each B,Al at *T*(3), there are up to 0.57 $^{M(1)}$Mg–$^{T(2)}$Si–$^{T(3)}$B,Al–$^{T(2)}$Si–$^{M(1)}$Mg clusters *pfu*. For each Si at *T*(3), there is insufficient Al at *T*(2) to produce the necessary 0.23 $^{M(1)}$Mg–$^{T(2)}$Al–$^{T(3)}$Si–$^{T(2)}$Al–$^{M(1)}$Mg clusters *pfu*. In this situation, there are two possibilities: (1) all $^{M(1)}$Mg–$^{T(2)}$Al–$^{T(3)}$Si–$^{T(2)}$Si–$^{M(1)}$Mg or a mixture of $^{M(1)}$Mg–$^{T(2)}$Al–$^{T(3)}$Si–$^{T(2)}$Al–$^{M(1)}$Mg and $^{M(1)}$Mg–$^{T(2)}$Si–$^{T(3)}$Si–$^{T(2)}$Si–$^{M(1)}$Mg.

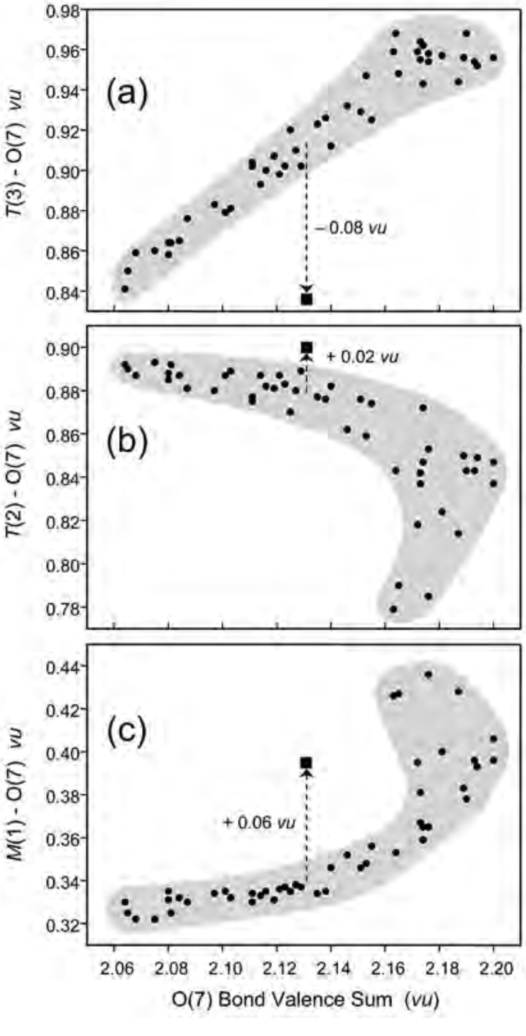

FIG. 5. Variation in individual bond-valences at the O(7) anion for the kornerupine structures of Cooper *et al.* (2009a). Data points are shown in black, and the fields of data are shaded grey for emphasis; data for K53 are shown as squares, and their displacement from the center of each field is marked by a broken arrow.

Consider next the arrangements involving O(8). For the arrangement Be–Al–Al–Al (Table 8), there is insufficient Al at *M*(2) for only this arrangement to occur. As $^{M(2)}$Al = 0.15 *apfu*, there could be up to 0.15 $^{T(3)}$Be–$^{M(2)}$Al–$^{M(5)}$Al–$^{M(5)}$Al and 0.05 $^{T(3)}$Be–$^{M(2)}$Mg–$^{M(5)}$Al–$^{M(5)}$Al configurations. If $^{M(2)}$Al were associated only with $^{T(3)}$Be, then the optimal arrangement involving $^{T(3)}$(B,Al) is 0.57 $^{T(3)}$(B,Al)–$^{M(2)}$Mg–$^{M(5)}$Al–$^{M(5)}$Al. The optimal arrangement involving Si at *T*(3) is $^{T(3)}$Si–$^{M(2)}$Mg–$^{M(5)}$Al–$^{M(5)}$Al , with only minor configurations involving Mg at *M*(5) owing to the low occupancy of *M*(5) by Mg.

Local variation in bond lengths and bond valences

The arguments developed in the above section were based solely on (Pauling) bond-strengths, which are dependent only on cation charge and cation coordination-number, and are independent of bond length. However, bond-valence theory (Brown 1981, Hawthorne 1994, 1997a) shows that there is a well-developed relation between bond valence and bond length. Hence one must expect local differences in crystallographically identical bond-lengths (and thus bond valences). Although such short-range features of a structure cannot be calculated directly, they may be deduced by comparing the long-range behaviors of bond lengths and bond valences in topologically identical structures with a range of bulk (and hence local) chemical compositions.

The kornerupine minerals are ideal in this respect, as Cooper *et al.* (2009a) have reported structural information on forty-seven kornerupine structures spanning the entire range of chemical composition. Thus we may compare the analogous information on Be-bearing kornerupine with these data to extract information on the local effect of Be on bond lengths. Figure 5 shows the variation in bond valence (Brown & Altermatt 1985) of the *T*(3)–O(7), *T*(2)–O(7) and *M*(1)–O(7) bonds as a function of the sum of the bond valence incident at O(7); Figure 6 shows the analogous information for the O(8) anion. The optimum short-range arrangement involving Be at *T*(3) and the O(7) anion is $^{T(3)}$Be–$^{T(2)}$Si–$^{M(1)}$Mg with an incident bond-strength sum of 1.83 *vu* (Table 8). In order to comply with the valence-sum rule (Brown 1981, Hawthorne 1994, 1997b), the bonds to O(7) in this cluster should shorten relative to their range of values in Be-free kornerupine (in which the optimum local arrangement have bond-strength sums close to those required by the valence-sum rule).

In Figure 5, it can be seen that the bond valence incident at O(7) shows a considerable range of values (2.06–2.20 *vu*), and it is only by considering this incident bond-valence *as a function of constituent individual bond-valences* that we can discern differences between the behavior of Be-free and Be-bearing kornerupine. With a lower-charge cation (Be) at *T*(3), one expects a much smaller *local* ${}^{T(3)}$Be–O(7) bond-valence (~0.50 *vu*), and hence a slightly smaller *long-range* *T*(3)–O(7) bond-valence than that in a Be-free kornerupine; Figure 5a shows that this is the case. Moreover, one may extract more quantitative information. The long-range *T*(3)–O(7) bond-valence is 0.08 *vu* lower in Be-bearing kornerupine K53 than in a Be-free kornerupine with the same bond-valence incident at O(7). There is 0.200 *Be pfu* in K53, and the result of this is to decease the aggregate bond-valence by 0.08 *vu*. Extrapolating to *T*(3) = 1.00 Be produces a change in *T*(3)–O(7) of 0.08 × 1.00 / 0.200 = 0.40 *vu*, with a resulting predicted ${}^{T(3)}$Be–O(7) bond-valence of 0.91 – 0.40 = 0.51 *vu*, close to the value expected [*i.e.*, the characteristic bond-valence of Be: 0.50 *vu* (Brown 1981, Hawthorne 1997b]. There is a compensatory strengthening of the *T*(2)–O(7) and *M*(1)–O(7) bonds (Figs. 5b, c) in order to satisfy the bond-valence requirements of the O(7) anion. A similar analysis for the O(8) anion (Figs. 6a, b, c) leads to a predicted ${}^{T(3)}$Be–O(8) bond valence of 0.78 – 0.06 × 5 = 0.48 *vu*, and compensatory strengthening of the *M*(2)–O(8) and *M*(5)–O(8) bonds. The predicted bond-valence sum around ${}^{T(3)}$Be is 0.51 × 2 + 0.48 × 2 = 1.98 *vu*, in accord with the valence-sum rule for full occupancy of *T*(3) by Be.

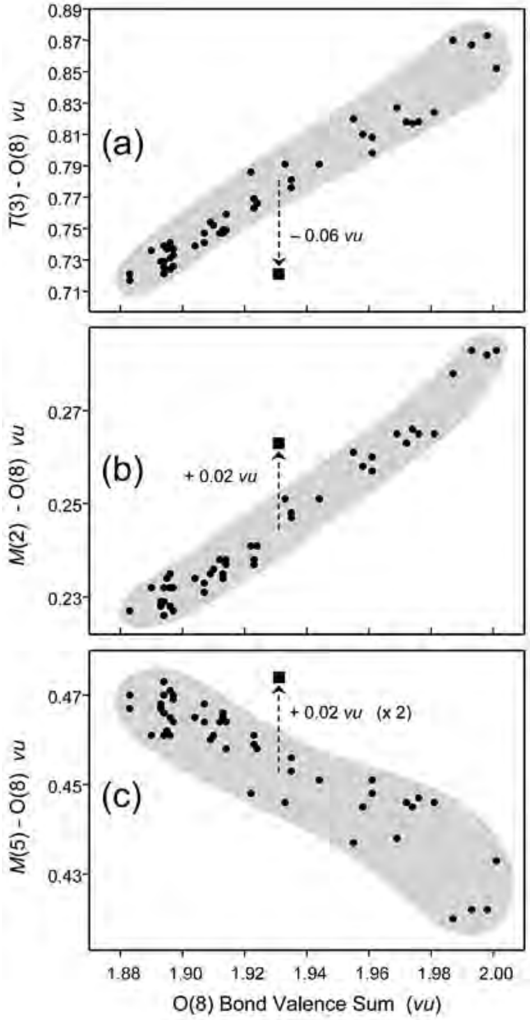

FIG. 6. Variation in individual bond-valences at the O(8) anion for the kornerupine structures of Cooper *et al.* (2009a). Data points are shown in black, and the fields of data are shaded grey for emphasis; data for K53 are shown as squares, and their displacement from the center of each field is marked by a broken arrow.

The incorporation of Be into kornerupine

It is clear from the results presented here that Be occurs only at the *T*(3) site in kornerupine. The other components of the *T*(3) site are B, Al and Si, all of which have a higher charge than Be, and hence the occurrence of Be at the *T*(3) site must be accompanied by additional heterovalent substitution within the structure. There are four possible such substitutions:

(1) Si → Al [particularly at *T*(2)]

(2) Al → Mg [particularly at *M*(2) and *M*(5)]

(3) Fe^{3+} → (Mg,Fe^{2+}) [at *M*(4)]

(4) (Mg, Fe^{2+}) → □ [at *X*]

All four substitutions are strongly linked to the maintenance of electroneutrality in the structure, and it is not possible to convincingly identify the relative importance of each substitution in the incorporation of Be at the *T*(3) site. However, only substitutions (1) and (2) satisfy local bond-valence requirements about the anions linked to Be, O(7) and O(8) (Figs. 4, 5 and 6), and hence we can discard substitutions (3) and (4) as possible candidates. Thus incorporation of Be into kornerupine must be accompanied by substitution of Si for Al at the *T* sites or substitution of Al for Mg at the *M* sites (or both).

ACKNOWLEDGEMENTS

We thank Gianni Andreozzi and Sergio Lucchesi for their helpful comments on this manuscript. This work was supported by a Canada Research Chair in Crystallography and Mineralogy and by Major Facilities Access, Equipment and Discovery Grants from the Natural Sciences and Engineering Research Council of Canada to FCH.

References

Azavant, P. & Lichanot, A. (1993): X-ray scattering factors of oxygen and sulfur ions: an *ab initio* Hartree–Fock calculation. *Acta Crystallogr.* **A49**, 91-97.

Brown, I.D. (1981): The bond-valence method: an empirical approach to chemical structure and bonding. *In* Structure and Bonding in Crystals II (M. O'Keeffe & A. Navrotsky, eds.). Academic Press, New York, N.Y. (1-30).

Brown, I.D. & Altermatt, D. (1985): Bond-valence parameters obtained from a systematic analysis of the inorganic crystal structure database. *Acta Crystallogr.* **B41**, 244-247.

Cooper, M.A., Hawthorne, F.C. & Grew, E.S. (2009a): The crystal chemistry of the kornerupine–prismatine series. I. Crystal structure and site populations. *Can. Mineral.* **47**, 233-262.

Cooper, M.A., Hawthorne, F.C., Grew, E.S. & Rossman, G.R. (2009b): The crystal chemistry of the kornerupine–prismatine series. II. The role of hydrogen. *Can. Mineral.* **47**, 263-274.

Grew, E.S. (1996): Borosilicates (exclusive of tourmaline) and boron in rock-forming minerals in metamorphic environments. *In* Boron: Mineralogy, Petrology and Geochemistry (E.S. Grew & L.M. Anovitz, eds.). *Rev. Mineral.* **33**, 387-502.

Grew, E.S. (2002): Beryllium in metamorphic environments (emphasis on aluminous compositions). *In* Beryllium: Mineralogy, Petrology, and Geochemistry (E.S. Grew, ed.). *Rev. Mineral. Geochem.* **50**, 487-549.

Grew, E.S., Chernosky, J.V., Werding, G., Abraham, K., Marquez, N. & Hinthorne, J.R. (1990a): Chemistry of kornerupine and associated minerals, a wet chemical, ion microprobe, and X-ray study emphasizing Li, Be, B and F contents. *J. Petrol.* **31**, 1025-1070.

Grew, E.S., Litvinenko, A.K. & Pertsev, N.N. (1990b): In search of whiteschists and kornerupine in the southwestern Pamirs, USSR. *Episodes* **13**, 270-274.

Grew, E.S., Pertsev, N.N., Vrána, S., Yates, M.G., Shearer, C.K. & Wiedenbeck, M. (1998): Kornerupine parageneses in whiteschists and other magnesian rocks: is kornerupine + talc a high-pressure assemblage equivalent to tourmaline + orthoamphibole? *Contrib. Mineral. Petrol.* **131**, 22-38.

Grew, E.S., Rao, A.T., Raju, K.K.V.S., Hejny, C., Moore, J.M., Waters, D.J., Yates, M.G. & Shearer, C.K. (2003): Prismatine and ferrohögbomite-2*N*/2*S* in granulite-facies Fe-oxide lenses in the Eastern Ghats Belt at Venugopalapuram, Vizianagaram district, Andhra Pradesh, India: do such lenses have a tourmaline-enriched lateritic precursor. *Mineral. Mag.* **67**, 1081-1098.

Grew, E.S., Yates, M.G., Barbier, J., Shearer, C.K., Sheraton, J.W. , Shiraishi, K. & Motoyoshi, Y. (2000): Granulite-facies beryllium pegmatites in the Napier Complex in Khmara and Amundsen Bays, western Enderby Land, East Antarctica. *Polar Geosci.* **13**, 1-40.

Hawthorne, F.C. (1994): Structural aspects of oxides and oxysalt crystals. *Acta. Crystallogr.* **B50**, 481-510.

Hawthorne, F.C. (1997a): Short-range order in amphiboles: a bond-valence approach. *Can. Mineral.* **35**, 201-216.

Hawthorne, F.C. (1997b): Structural aspects of oxide and oxysalt minerals. *In* Modular Aspects of Minerals (S. Merlino, ed.). *Eur. Mineral. Union, Notes in Mineralogy* 1, 373-429.

Hölscher, A. (1987): *Experimentelle Untersuchungen im System* $MgO–BeO–Al_2O_3–SiO_2–H_2O$*: Mg–Al-Surinamite und Be-Einbau in Cordierit und Sapphirin.* Ph.D. dissertation, Ruhr-Universität Bochum, Germany.

Ibers, J.A. & Hamilton, W.C., eds. (1992): *International Tables for X-ray Crystallography* IV. Kynoch Press, Birmingham, U.K.

Shannon, R.D. (1976): Revised effective ionic radii and systematic studies of interatomic distances in halides and chalcogenides. *Acta Crystallogr.* **A32**, 751-767.

Vrána, S. & Barr, M.W.C. (1972): Talc – kyanite – quartz schist and other high-pressure assemblages from Zambia. *Mineral. Mag.* **38**, 837-846.

Received March 16, 2006, revised manuscript accepted April 3, 2009.

APPENDIX

In Figure 1, the data for K53 were forced to fit the relations developed for $T(1)$ and $T(2)$ in Be-free kornerupine, with the result that the data for $T(3)$ in K53 deviates significantly from the data for Be-free kornerupine (Fig. 1c). It could be argued that constraining the $T(1)$ and $T(2)$ data in K53 to agree *exactly* with the linear relations developed in Figures 1a and 1b has exaggerated the deviation of K53 from the linear relation in Figure 1c, particularly as the multiplicities of the $T(1)$ and $T(2)$ sites are each twice that of the $T(3)$ site, and small coupled lateral displacements of points on the $T(1)$ and $T(2)$ plots would result in significant readjustments to the point on the $T(3)$ plot. We will now examine this possibility in detail.

If we replace some Si by Al at the $T(3)$ site in K53, the point for K53 in Figure 1c would be appreciably closer to the ideal relation as $^{[4]}$Al (r = 0.39 Å) is substantially larger than Si (r = 0.26 Å; radii from

Shannon 1976). This would have a negligible effect on the amount of B derived from site-scattering refinement, as Si and Al have very similar X-ray scattering factors (Z = 14 and 13, respectively), whereas B has a very different X-ray scattering factor (Z = 5). In order to retain the correct amount of Si at the *T* sites (Table 2), we would have to increase the amount of Si at *T*(1) or *T*(2) (or both) and reduce the corresponding amount of $^{[4]}$Al. This cumulative readjustment is shown in Figure A1, in which reasonable variations for data from Be-free kornerupine are indicated by the shaded fields; the resultant site-populations are shown in Table A1. The modified data for K53 almost fall within the shaded region, and one might be tempted to dismiss the likelihood of a significant fourth component (*i.e.*, Be) at *T*(3) in order to account for the observed stereochemistry. However, the kornerupine structure involves a complex interplay of Si–Al order over the tetrahedral sites, partly in response to various B contents. This is shown in Figure A2 for the *T*(3) site; the data for the 47 kornerupine crystals of Cooper *et al.* (2009a) plot within the shaded field, showing that the Si:Al ratio is constrained within fairly narrow limits for a specific B content. The initial *T*-site assignments (Table 4) result in data point 1, and the readjusted *T*-site assignments (Table A1) result in data point 2. The redistribution of Si and Al over the *T*

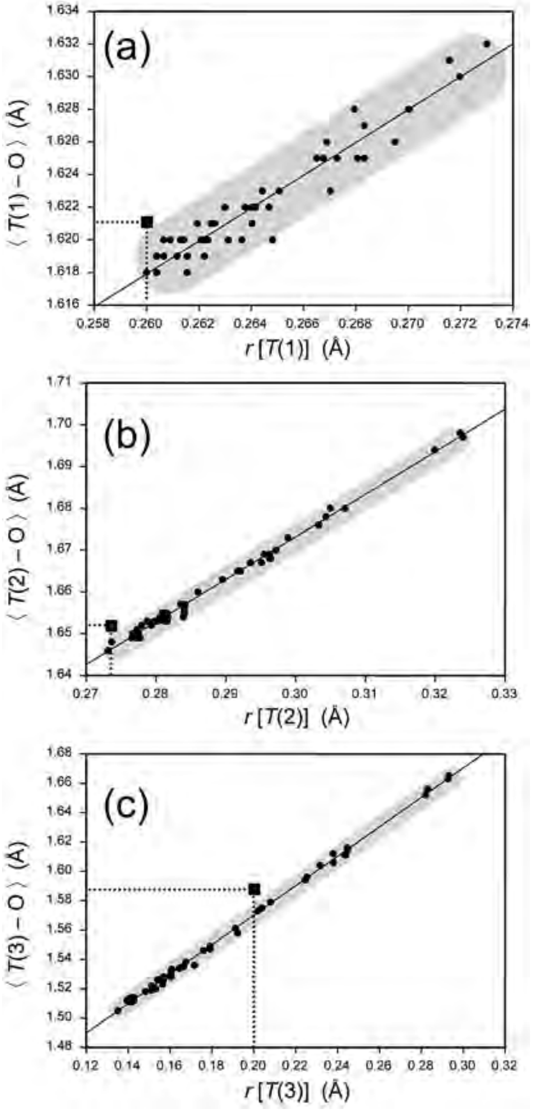

FIG. A1. The variation in <*T*–O> distances a function of constituent-cation radius for the data of Cooper *et al.* (2009a) (black circles) and for K53 (Table A1) (squares); also shown are the regression lines of Cooper *et al.* (2009a). The shaded fields denote the possible range of data that would agree with the regression lines.

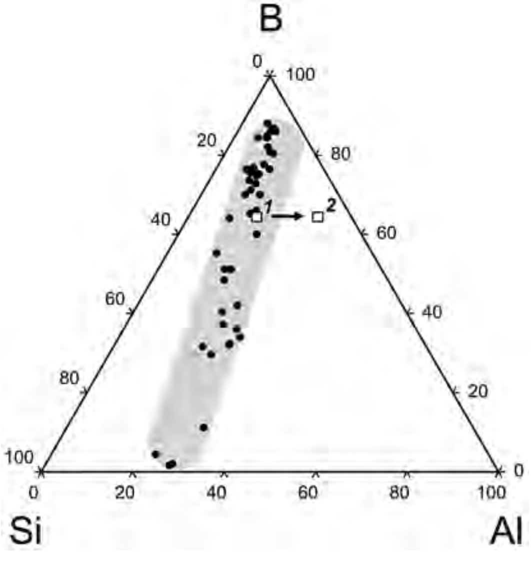

FIG. A2. The variation in Si, Al and B at the *T*(3) site in the kornerupine structures of Cooper *et al.* (2009a); legend as in Figure A1. For K53, data point 1 represents the initial *T*-site assignment, and data point (2) represents the readjusted *T*-site assignments shown in Table A1.

TABLE A1. ADJUSTED SITE-POPULATIONS FOR KORNERUPINE K53

	Si	Al	B	r (Å)
T(1)	2.000	0.000	–	0.260
T(2)	1.791	0.209	–	0.274
T(3)	0.074	0.282	0.644	0.200

sites, which was done in order to minimize the overall deviations for K53 on Figure A1, results in an Si–Al content at *T*(3) that is in glaring discord with the results of Cooper *et al.* (2009a). A distribution of Si, Al and B over *T*(1), *T*(2) and *T*(3) conformable with established kornerupine site-populations is not possible for K53. Disregarding gross analytical error, we can therefore conclude that a fourth component is present (in appreciable quantity) at the *T* sites in kornerupine K53.